

# A mixed basis with off-center Gaussian functions for the calculation of the potential energy surfaces for $\pi$ -stacking interactions: dimers of benzene and planar $C_6$

Ersin Yurtsever

Received: 8 September 2014 / Accepted: 7 December 2014 / Published online: 22 January 2015  
© Springer-Verlag Berlin Heidelberg 2015

**Abstract** A practical mixed basis set was developed to facilitate accurate calculations of potential energy surfaces for  $\pi$ -stacking interactions. Correlation consistent basis sets (cc-PVXZ) were augmented by p-type Gaussian functions placed above and below the planes of  $C_6$  moieties. Møller-Plesset (MP2, SCS-MP2) and coupled cluster [CCSD(T)] calculations show that such generated basis sets provide an accurate description of  $\pi$ -stacking systems with favorable computation times compared to the standard augmented basis sets. The addition of these off-center functions eliminates the linear dependence of the augmented basis sets, which is one of the most encountered numerical problems during calculation of the oligomers of polyaromatic hydrocarbons (PAH). In this work, we present a comparative study of the general characteristics of the potential energy surfaces for the parallel stacked and T-shape conformations of benzene and planar  $C_6$  clusters, using a combination of cc-PVXZ and our optimized functions. We discuss properties, such as the depth and curvature of the potential functions, short and long distance behavior, and the frictional forces between two model monomers.

**Keywords** Stacking interactions · CCSD · Basis set

## Introduction

One of the important challenges of quantum chemical methods has been the correct description of long-range

interactions. Although long-range interactions were originally thought to be responsible mostly for solid state structures, there are numerous cases where the physics and chemistry of relatively small systems are also governed by such long-range forces. These forces may result in the formation of molecular aggregates, without actually breaking or forming new chemical bonds. Since the aggregates are kept together with relatively weaker forces compared to covalent bonds, the phrase “noncovalent interaction” is now commonly accepted as a keyword defining this computationally challenging phenomenon. Noncovalent interactions can be detected between different molecules, as well as between the segments of a large molecule. They define the shape, stability and dynamics of the system.

Hydrogen bonds are the most common example of noncovalent interactions and they have been studied extensively since the beginning of the twentieth century [1]. The interest in hydrogen-bonding was due mostly to its important role in the majority of biologically important processes, such as the conformational stability of nucleic acids [2], and the structure and dynamics of RNA [3]. Most drug design problems are associated with various types of hydrogen bonding [4]. The presence and strength of these bonds can be used to explain both the molecular structures and the dynamics of these systems. Hydrogen bonds also play an important role in the morphology of macromolecules where some of the constituents form either inter- or intra-chain hydrogen-bonds, hence affecting the stability and the mechanical properties of polymers [5]. For all these problems, standard quantum chemical methods could give accurate assessments of the interactions between small segments and provide guidelines for the conformational stability of large systems. These results can also be used to develop reasonably correct force fields for molecular simulations of aggregations. The types of the interactions mentioned here are somewhat longer than chemical bonds, but still within the realm of Hartree-Fock (HF) or

E. Yurtsever (✉)  
Chemistry Department, Koç University, Rumelifeneriyolu, Sariyer,  
Istanbul 34450, Turkey  
e-mail: eyurtsev@ku.edu.tr

density functional theory (DFT) methodologies. Reasonable geometries and bond strengths can be obtained with small basis sets. However, longer range hydrogen bonds [6] still require computationally more expensive methods. Here, especially orthodox DFT techniques suffer from their inadequate description of long-range interactions.

Another set of computationally challenging problems associated with the presence of long-range interactions is so-called “ $\pi$ -stacking” or, more generally, “stacking” systems [7]. One of the two potentially important areas is the  $\pi$ -stacking of amino acids. Crystal structures of stable protein dimers reveal both parallel and T-shaped conformations, when aromatic or pseudo-aromatic constituents are present. These structures are thought to be due to the presence of stacking-type interactions. Similarly, various aggregates of polycyclic aromatic hydrocarbons (PAH) are stabilized by  $\pi$ -stacking. The growing interest in the possible applications of functionalized forms of graphenes, graphones and graphanes [8] makes the study of  $\pi$ -stacking a highly attractive problem.

In both sets of problems, the relative weakness of interactions coupled with the longer distances between constituents, require more accurate and careful calculations than the conventional ab-initio or DFT methods used commonly for the study of organic reaction mechanisms [9, 10]. For example, the most commonly used DFT functionals, such B3LYP, find the stacking interaction between two benzene molecules as repulsive, when the actual interaction is small but attractive. In fact, the majority of DFT functionals perform poorly in predicting noncovalent interactions. There have been numerous attempts to define broadly applicable functionals that could work for long-range interactions [11, 12]. Even though it is possible to develop tailored functionals for a specific set of compounds, the dependence of the results on the choice of a functional form is not a reliable concept/approach. Another strategy is the modification of DFT methods for a better description of the long term behavior of interactions. There are examples, such as symmetry-adapted-perturbation-theory (DFT-SAPT) [13] or dispersion-corrected DFT (DFT-D) [14]; however, in this work, we have restricted ourselves to the comparison of ab-initio based methods.

Ab-initio calculations excluding the correlation terms seem to perform as poorly as DFT in predicting noncovalent interactions. Similar to the DFT case with B3LYP functional, the potential energy curve for the dimerization of benzene in sandwiched form obtained from HF/6-31(d) is purely repulsive. For hexa-peri-hexabenzocoronene (HBC), which forms disc-like structures, HF and DFT methods using small basis sets give repulsive potential energy functions. Ab-initio calculations including the correlation energy seem to work much better than HF and DFT, although in this case they are highly demanding computationally. The most economical of these methods is MP2; however, it has been shown on many occasions that MP2 overemphasizes the strength of the interaction

and the bond lengths tend to be shorter than those calculated with more sophisticated methods. One of the modifications of standard MP2, the so-called spin-component-scaled MP2 (SCS-MP2), seems able to correct this major error in the MP2 method [15]. Here, the energy of a closed-shell molecule is calculated as a mixture of the singlet and the triplet states with appropriate weights. In the standard case, these weights are taken as two-thirds and one-third, respectively. Upon applying these corrections, we observe that most of the characteristics of the potential energy surfaces improve drastically. Of course, the most reliable results come from the coupled cluster calculations including single, double and triple excitations. We have noticed that the exclusion of triples affects the numerical results strongly and in a negative way. The drawback to this approach/strategy is the cost of the computations and, consequently, only a few calculations on larger molecules have been carried out.

An oft-encountered numerical problem with the non-covalent interactions within PAH stacking is the linear dependence of the basis sets. The majority of the post-HF calculations use correlation-consistent basis sets, which are denoted as cc-pVXZ, where X can be from 2 to 6. The X value coming from Slater-type-function formalism defines basis sets known as double-zeta, triple-zeta, etc. Even though these basis sets provide very good geometrical parameters and energetics around the minimum energy conformations, they need to be augmented by diffuse functions to study long-range interactions. There are standard extensions under the common notation of aug-cc-pVXZ, as well as several other modified forms. These extended basis sets do correct the long-range behavior of interactions, but come at a quite large computational cost. One of the major complications of using the augmented basis sets is that they quite often produce linearly dependent basis functions when applied to stacked dimers of relatively large PAHs, such as triphenylene [16] or coronene.

## Methods

In this work, we present a simple augmentation of the standard cc-pVXZ basis sets, which is both computationally inexpensive and generates linearly independent basis sets.

In the early days of quantum chemical theory, the idea of using Gaussian functions located not on atoms but in different points in space was tried and found to be computationally efficient [17, 18]. But the lack of simple rules to generate such basis functions has slowly reduced the advantages of these floating Gaussian orbitals (FGO). Another similar approach (mid bond functions) has been used to calculate highly accurate potential energy functions, where additional Gaussian functions are placed at the center of the bonds [19, 20].

We used the FGO concept to generate a mixed basis set that linearly independent and could generate potential energy

surfaces economically. The linear dependence of the augmented basis sets comes mostly from the small-exponent p-functions placed in the molecular plane. The computationally challenging part of non-covalent interactions are in the space between different constituents. Therefore, in a fashion similar to mid-bond functions, we could carry out accurate but more economical calculations by placing these additional functions above (and below) the molecular planes. Unlike FGOs and midbond functions, which depend on the geometry of the complex, our functions are placed on fixed positions relative to the molecular planes and are not reoptimized for the conformation of the complex.

We used this mixed basis set to calculate interactions between benzene and planar  $C_6$  dimers. The calculations cover short and long distances at the sandwiched and T-shaped conformers. We also calculated the frictional forces within the dimers of these two model monomers.

## Results and discussion

We chose benzene and the planar ring conformation of  $C_6$  to model interactions between PAHs and graphene sheets. The cyclic  $C_6$  cluster is a stable structure with an energy 8 kcal mol<sup>-1</sup> above the linear cluster [21].  $C_6$  may not be a sufficiently good model for a graphene sheet; however, our aim was to study the effects of these basis sets and dependence of physical properties to the various augmentation schemes. For benzene geometry, we used  $R(C=C)=1.3915$  Å and  $R(C-H)=1.08$  Å. For the planar ring structure of  $C_6$ ,  $R(C-C)=1.317$  Å was used. Bond lengths were obtained from optimizations with MP2/aug-cc-pVDZ basis sets preserving  $D_{6h}$  symmetry in both molecules. These geometrical parameters were kept constant during the calculations.

We started with the standard cc-pVXZ basis sets and added off-center Gaussian functions to obtain various augmentations. There are a number of possibilities for positioning these functions to generate a mixed basis set. The number of Gaussian functions, type of function (s,p or d-type), exponents and positions can be tuned to get the most economical, but a still accurate set.

We used the stacked benzene dimer as our reference system and optimized the above mentioned parameters. Firstly, we decided to employ p-functions only, as s-functions did not seem to contribute significantly to the interaction energy and d-functions increased the computational cost. For each molecule, Gaussian functions were placed on two planes above and below the molecular plane. Considering the positions of the functions above the plane, the simplest choice was placing a single function at the center. Alternatively, we tried three Gaussians placed on the corners of an equilateral triangle or six Gaussians placed above each carbon atom. These augmentations are denoted as cc-pVXZ + 2, cc-pVXZ + 6 and cc-

pVXZ + 12 throughout the manuscript. By simple optimizations, we found that, with the cc-pVXZ + 6 basis, the sides of the equilateral triangle is 0.65 Å, which is 0.75 Å away from the molecular plane. Similarly with the cc-pVXZ + 12 basis, centers of the basis functions are 0.75 Å above and below each carbon atom. In all cases, the exponent of the p-type Gaussian was chosen as  $\zeta=0.2$ . Neither cc-pVXZ + 2 nor cc-pVXZ + 6 contributed significantly to the interaction energies, whereas cc-pVXZ + 12 basis sets drastically improved the quality of characteristics of the potential energy functions. Most importantly, this mixed basis set was found to be linearly independent and thus we did not encounter any convergence problems.

The calculations were carried out with MOLPRO 2010.1-13 [22] and off-center Gaussians were placed using the dummy atom formalism. Basis set superposition errors (BSSE) were corrected by the counterpoise method of Boys [23]. Table 1 presents results of the stacked  $C_6$  dimer (sandwich form) with SCS-MP2 method and increasing augmentation levels. Here, we restricted ourselves to SCS-MP2 in order to generate a large set of test results with larger basis sets. The results from the standard augmented basis sets are also included for comparison. For the smaller basis sets of cc-pVDZ and cc-pVTZ, the potential energy functions were calculated within the range of  $3. \text{Å} < R < 10 \text{Å}$ , where  $R$  represents the vertical separation between two  $C_6$  monomers. In Table 1, the number of primitive Gaussian functions and number of contractions are given as measures of the complexity of the calculations. The minima of the potential (in Å), depth of the potential well (in kcal mol<sup>-1</sup>), curvature at the minima ( $[\text{kcal mol}^{-1} (\text{Å})^{-2}]$ ,  $R_i$  where the second derivative is zero (in Å), are given for all basis sets tested. The effects of the basis sets on short-range behavior were checked by fitting the interaction potentials to simple power laws as  $V=R^{-n}$ . This  $n$  is given in the table as the repulsive power. The long range of the potential functions behaved almost uniformly as  $R^{-6}$  and they are not included in the table. Complete basis set extrapolations were also employed to calculate  $R_{\min}$  and  $V_{\min}$  with three data points. HF energies were extrapolated by:

$$E = E_{\text{CBS}} + A e^{-(n-1)} + B e^{-((n-1)*(n-1))} \quad (1)$$

Here  $n$  is the cardinal number for the basis set such as  $n=2$  for cc-pVDZ, etc. Correlation energies were extrapolated as in the default mode of Molpro, which is given in Eq. 2.

$$E = E_{\text{CBS}} + A n^{-3} \quad (2)$$

Again,  $n$  describes the cardinal number of the basis set. At each  $R$  value, energies of both the fragments and the supermolecule were calculated with same basis sets and then

**Table 1** Spin-component-scaled second-order Møller-Plesset (SCS-MP2) results for sandwich dimer of  $C_6$ .  $R_{\min}$  and the inflection points are in Å,  $V_{\min}$  are in kcal mol $^{-1}$  and the curvature is in kcal mol $^{-1}$  Å $^{-2}$ 

Basis set	Primitive functions	Contractions	$R_{\min}$	$V_{\min}$	$V''(R_{\min})$	$R(V''=0)$	Repulsive power
d	324	168	3.842	1.821	9.6	4.28	14.7
d+2	336	180	3.798	2.218	9.2	4.24	15.3
d+6	360	204	3.737	2.800	13.6	4.20	16.2
d+12	396	240	3.723	3.096	13.8	4.19	16.4
ad	444	276	3.731	3.096	13.8	4.20	16.2
t	564	360	3.743	2.738	13.4	4.21	16.0
t+2	576	372	3.723	2.944	13.2	4.19	16.4
t+6	600	396	3.698	3.185	12.6	4.17	16.2
t+12	636	432	3.687	3.346	12.5	4.16	16.4
at	804	552	3.688	3.369	12.4	4.17	16.2
q	996	660	3.694	3.184	12.2		
q+2	1,008	672	3.685	3.282	12.3		
q+6	1,032	696	3.670	3.411	12.2		
q+12	1,068	732	3.670	3.469	12.2		
aq	1,416	960	3.662	3.509	11.9		
CBS			3.676	3.305			
CBS+2			3.672	3.372			
CBS+6			3.664	3.449			
CBS+12			3.665	3.513			
aug-CBS			3.651	3.557			

extrapolations were carried out for fragments as well. CBS notation is used for extrapolations from cc-pVDZ, cc-pVTZ and cc-pVQZ basis sets, while CBS + 12 implies the extrapolations from cc-pVDZ + 12, cc-pVTZ + 12 and cc-pVQZ + 12 basis sets.

In the tables and figures, we used the notation such that d, d2, d6, d12 and ad represent cc-pVDZ, mixed basis sets with 1, 3 or 6 off-center Gaussians on each side and aug-cc-pVDZ, respectively.

For a better comparison of the quality of the basis sets, we plotted the potential energy functions of cc-pVTZ, cc-pVTZ +

12 and aug-cc-pVTZ sets in the range of 3.0 Å–5.0 Å (Fig. 1). It can be seen clearly that the use of off-center Gaussians is equivalent to the augmented basis sets with a marginal computational mark up from cc-pVTZ basis.

For the value of the potential depth, we saw that the introduction of off-center Gaussians recovered 80 % of the energy difference between cc-pVXZ and aug-cc-pVXZ basis sets, as well as that of the CBS limit. This comes from adding only a small and fixed number of primitives. The additional computational cost becomes less and less significant as the basis is increased from  $X=2$  to  $X=4$ . Values of  $R_{\min}$  are also much closer to the standard augmented basis sets.

The parameters of the potential energy functions can be calculated reasonably well for all mixed basis sets, whereas cc-pVXZ alone performs poorly. The curvature at  $R_{\min}$  was either too low for  $X=2$  or too high for  $X=3$ , while our results are close to those obtained from corresponding aug-cc-pVXZ sets. Similarly, our basis sets produced the inflection points and the power law exponent of the repulsive wall of augmented basis sets accurately.

In Table 2, we present a different comparison of results from the  $C_6$  dimer sandwich. The properties of the potential energy functions are given for MP2, SCS-MP2, CCSD and CCSD(T) with and without augmented basis sets.

As these Gaussians are placed above and below the planes of molecules, one could question the validity of such an augmentation for dimers other than the sandwich

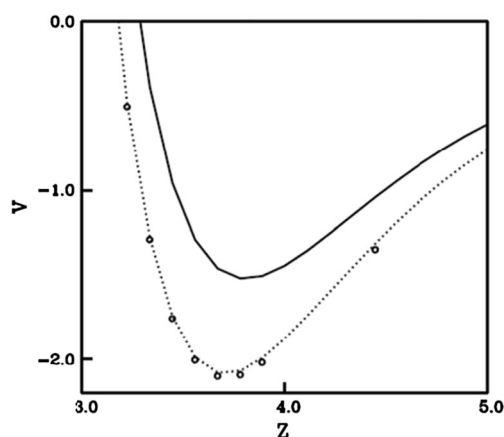


**Fig. 1** Potential energy for parallel stacked  $C_6$  dimer. Solid line vt, dotted line t12, circles at

**Table 2** Comparison of methods and basis sets for C<sub>6</sub> dimer sandwich

	d	d+12	ad	t	t+12	at
$R_{\min}$ (Å)						
MP2	3.677	3.561	3.576	3.580	3.526	3.525
SCS-MP2	3.842	3.723	3.723	3.743	3.687	3.688
CCSD	4.273	4.034	4.051	4.114	4.024	3.816
CCSD(T)	4.068	3.867	3.884	3.931	3.840	3.843
$V_{\min}$ (kcal mol <sup>-1</sup> )						
MP2	3.023	4.940	4.923	4.423	5.362	5.395
SCS-MP2	1.821	3.096	3.096	2.739	3.346	3.369
CCSD	0.517	1.211	1.171	0.917	1.250	1.278
CCSD(T)	0.861	1.965	1.931	1.526	2.090	2.110
$V''(R_{\min})$ (kcal mol <sup>-1</sup> /Å <sup>2</sup> )						
MP2	12.0	16.8	17.6	16.4	24.0	23.5
SCS-MP2	9.6	13.8	14.1	13.5	12.5	12.4
CCSD	1.6	5.9	3.8	4.0	5.5	1.3
CCSD(T)	3.0	7.1	7.2	7.4	10.1	10.1
$R(V''=0)$ (Å)						
MP2	4.11	4.04	4.05	4.06	4.00	5.06
SCS-MP2	4.28	4.19	4.20	4.21	4.16	4.19
CCSD	4.78	4.49	4.53	4.57	4.50	5.54
CCSD(T)	4.53	4.33	4.35	4.39	4.31	5.32
Repulsive power						
MP2	17.6	21.1	20.5	20.4	22.8	22.9
SCS-MP2	14.7	16.4	16.2	16.0	17.3	17.2
CCSD	11.8	12.6	12.6	12.1	12.8	12.7
CCSD(T)	12.8	14.2	14.0	13.5	14.6	14.5

conformation. As the benzene dimer has a global minimum at the T-shaped structure, we tested this basis set for a T-shaped C<sub>6</sub> dimer. The results of this structure are given in Table 3 and Fig. 2. The distance Z is defined as the distance between the center of masses of each monomer. Unlike benzene, the T-shaped conformer of C<sub>6</sub> is 0.8 kcal mol<sup>-1</sup> less stable than the sandwich conformer.

Using aug-cc-pVTZ results from CCSD(T) as our benchmark, we observed several trends. The most striking result is that CCSD without the triples gives consistently poor results in all regions of the potential energy function. Binding energies and  $V''(R_{\min})$  are too low, in case of the T-shaped dimer  $R_{\min}$  is also too small by 0.85 Å. Repulsive region of the interaction is found to be slightly less steeper.

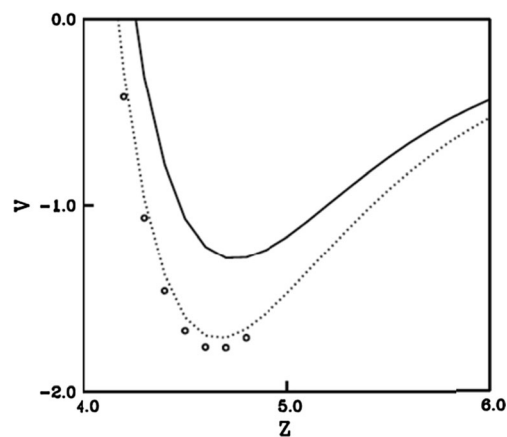
It is a well known fact that MP2 overemphasizes the interaction and we note that binding energies are 2.5–3.2 kcal/mol<sup>-1</sup> too high, although  $R_{\min}$  is located reasonably correctly. In a similar fashion, curvature of the potential energy around the minimum is 2–3 times higher. Another failure of the MP2 is at the repulsive wall of the potential, where the repulsive power is found to be too high. SCS-MP2 seems to change the characteristics of the potential energy curves in the

**Table 3** Comparison of methods and basis sets for T-shaped dimer of C<sub>6</sub><sup>a</sup>

	D	d+12	ad	t	t+12	at
$R_{\min}$ (Å)						
MP2	4.548	4.411	4.419	4.401	4.354	4.343
SCS-MP2	4.723	4.569	4.584	4.580	4.528	4.513
CCSD	5.070	4.866	4.894	4.932	4.845	3.800
CCSD(T)	4.898	4.705	4.724	4.747	4.668	4.656
$V_{\min}$ (kcal mol <sup>-1</sup> )						
MP2	2.216	3.813	3.830	3.492	4.194	4.333
SCS-MP2	1.351	2.403	2.412	2.141	2.628	2.703
CCSD	0.484	1.008	1.013	0.797	1.056	1.177
CCSD(T)	0.763	1.599	1.614	1.290	1.716	1.772
$V''(R_{\min})$ (kcal mol <sup>-1</sup> /Å <sup>2</sup> )						
MP2	11.4	14.4	15.0	13.2	12.9	18.8
SCS-MP2	6.2	8.1	8.3	7.5	10.6	10.6
CCSD	1.7	3.6	3.7	3.6	5.0	0.2
CCSD(T)	3.3	6.5	6.7	6.3	5.8	5.6
$R(V''=0)$ (Å)						
MP2	5.00	4.90	4.91	4.89	4.85	5.87
SCS-MP2	5.17	5.06	5.08	5.07	5.01	5.89
CCSD	5.53	5.34	5.38	5.40	5.33	5.96
CCSD(T)	5.34	5.18	5.21	5.23	5.15	5.91
Repulsive power						
MP2	19.4	23.7	23.3	24.3	26.2	27.0
SCS-MP2	16.7	19.0	18.8	19.0	20.1	20.4
CCSD	13.9	15.1	14.9	14.6	15.3	15.1
CCSD(T)	15.0	16.8	16.5	16.2	17.3	17.5

<sup>a</sup> All distances are in terms of the distances between center of masses of two molecules (Å)

right direction. Binding energies and  $V''(R_{\min})$  were lowered and  $R_{\min}$  was much closer to the CCSD(T) results. The steepness of the repulsive wall was corrected to a great extent.

**Fig. 2** Potential energy for T-shaped C<sub>6</sub> dimer. Solid line vt, dotted line t12, circles at

For all methods described here, our augmented basis sets compare very well with the standard augmentations. From the figures, one can see that the differences between the potential energy curves are very small even for the T-shaped conformer. The only noticeable difference is in the location of the point where  $V''=0$ . Our augmentation locates that point  $0.7 \text{ \AA} - 1.0 \text{ \AA}$  too short. Considering all the parameters presented here, we can safely conclude that the augmentation works almost equally well for both dimers by capturing the long range interactions between monomers correctly.

The calculations are repeated for both sandwich and T-shaped conformations of benzene. They are presented in Table 4 and Fig. 3. It is interesting to note that the CCSD with basis set of cc-pVDZ gives a purely repulsive curve for the parallel conformer. Overall, the addition of off-center

Gaussians change the characteristics of the potential energy in the correct direction. The previously reported highly accurate calculations of Pulay [24] gives the benzene-benzene distances and the interaction energies of sandwich and T-shaped dimers as  $3.92 \text{ \AA}$ ,  $4.99 \text{ \AA}$ ,  $1.65 \text{ kcal mol}^{-1}$  and  $2.68 \text{ kcal mol}^{-1}$ , respectively.

These results convinced us that the use of SCS-MP2 and augmentation of the cc-pVTZ basis with 12 off-center Gaussians per six-membered ring could be an economically viable way to understand long-range stacking interactions for larger systems.

To further illustrate this approach, we calculated the frictional forces between two planar  $C_6$  and two benzene rings at various intermonomer distances. Force was calculated as the negative numerical derivate of the potential. Even though it

**Table 4** Comparison of methods and basis sets for sandwich and T-shaped benzene dimers<sup>a</sup>

	Sandwich				T-shaped			
	D	ad	t	t+12	d	ad	t	t+12
$R_{\min}$ (Å)								
MP2	3.935	3.747	3.761	3.714	5.080	4.946	4.913	4.889
SCS-MP2	4.266	3.934	3.951	3.902	5.225	5.097	5.068	5.037
CCSD	Repulsive	4.144	4.204	4.120	5.285	5.149	5.141	5.106
CCSD(T)	4.398	3.963	4.007	3.929	5.214	5.065	5.044	5.010
$V_{\min}$ (kcal mol <sup>-1</sup> )								
MP2	1.024	2.917	2.484	3.147	1.956	3.080	2.981	3.308
SCS-MP2	0.346	1.544	1.242	1.682	1.348	2.107	2.009	2.244
CCSD	Repulsive	0.694	0.396	0.736	1.166	1.839	1.694	1.910
CCSD(T)	0.192	1.390	0.997	1.514	1.390	2.315	2.138	2.455
$R(V=0)$ (Å)								
MP2	3.509	3.274	3.295	3.234	4.567	4.417	4.377	4.355
SCS-MP2	3.818	3.473	3.510	3.435	4.711	4.568	4.548	4.515
CCSD	Repulsive	3.706	3.821	3.684	4.775	4.627	4.620	4.584
CCSD(T)	3.969	3.502	3.575	3.469	4.702	4.541	4.529	4.488
$V''(R_{\min})$ (kcal mol <sup>-1</sup> /Å <sup>2</sup> )								
MP2	6.2	15.5	9.7	14.2	6.6	12.8	11.2	11.0
SCS-MP2	1.5	8.2	5.2	7.7	5.4	7.0	6.0	9.1
CCSD	Repulsive	4.4	3.0	4.3	3.9	7.8	6.9	6.8
CCSD(T)	1.0	5.4	5.6	8.0	5.4	7.0	9.1	9.0
Repulsive power								
MP2	18.1	22.8	22.4	25.0	20.8	24.7	17.1	22.9
SCS-MP2	14.5	17.3	16.8	18.0	18.2	20.5	15.4	19.3
CCSD	12.3	14.4	13.8	14.5	17.5	19.4	14.8	18.2
CCSD(T)	13.8	16.7	16.0	17.3	18.4	21.2	15.5	19.8
$R(V''=0)$ (Å)								
MP2	4.37	4.21	4.22	4.19	5.56	5.45	5.42	5.39
SCS-MP2	4.79	4.39	4.41	4.19	5.70	5.59	5.57	5.54
CCSD	5.23	4.60	4.61	4.19	5.76	5.65	5.65	5.60
CCSD(T)	4.93	4.43	4.44	4.19	5.69	5.56	5.55	5.50

<sup>a</sup> All distances are in terms of the distances between center of masses of two molecules (Å)

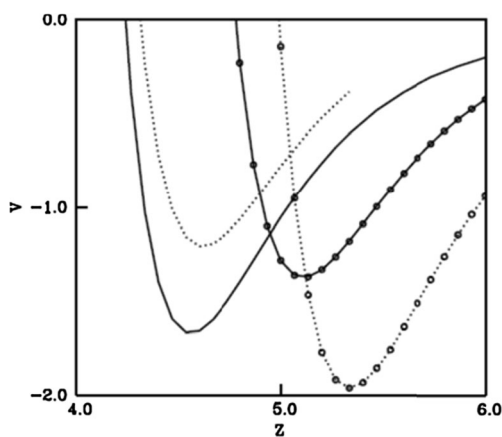


**Fig. 3** Potential energy functions with CCSD(T) and basis t12. *Solid line* Sandwich  $C_6$ , *solid lines with circles* T-shaped  $C_6$ , *dotted line* parallel  $C_6H_6$ , *dotted line with circles* T-shaped  $C_6H_6$

was obtained numerically, the frictional force is a more sensitive measure of the small changes in the wavefunction than the potential itself. A quick study of basis sets showed that the resulting forces from aug-cc-pVTZ and cc-pVTZ + 12 were almost identical. Therefore, the results presented in Figs. 4 and 5 were obtained from FGO augmentation basis sets with SCS-MP2.

We began with a sandwich conformation of two monomers and dragged one of them along an axis connecting two carbon atoms. The potential energy function along this reaction coordinate ( $\delta x$ ) was recorded and the frictional forces were calculated numerically. This process was repeated at several vertical monomer–monomer distances ( $z$ ). The smallest distance chosen was 3.1 Å for  $C_6$  and 3.0 Å for benzene. Several potential curves were then calculated at 0.2 Å intervals in  $z$ . This range was chosen so that geometry-dependent fluctuations of the forces could be detected. In Figs. 4 and 5 the frictional forces are plotted at different intermonomer distances.

For the  $C_6$  dimer, above  $z=3.7$  Å, the interaction was very weak and the most stable conformer was nearly the sandwich

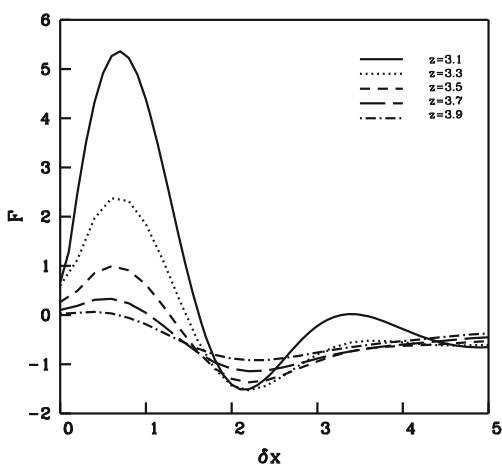


**Fig. 4** Frictional forces for  $C_6$ ,  $\delta x$  in Å and  $F$  in ( $\text{kcal mol}^{-1} \text{Å}^{-1}$ )

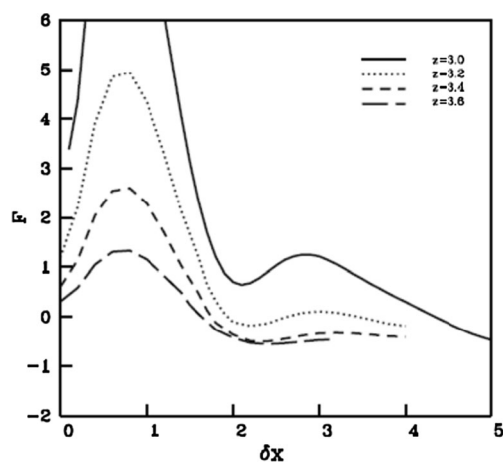


**Fig. 5** Frictional forces for  $C_6H_6$ ,  $\delta x$  in Å and  $F$  in ( $\text{kcal mol}^{-1} \text{Å}^{-1}$ )

one. Actually, the displaced conformer still had lower energy; however, the force was nearly zero. As  $z$  decreased, the displacement of the minimum energy conformer became larger. For  $z=3.1$  Å, the minimum energy was observed at  $\delta x=1.6$  Å with an energy difference of 3  $\text{kcal mol}^{-1}$  compared to the parallel stacked conformer. A rough estimate of the global minimum occurs at  $z=3.5$  Å and  $\delta x=1.2$  Å.

In the case of benzene, below  $z=3.2$ , the minimum corresponds to a highly displaced structure where  $\delta x=3-4$  Å. As  $z$  increased, first a double minimum character was observed as in  $z=3.0$  Å and then the known displaced structure was found [24, 25].

## Conclusions

We have developed a mixed basis set by augmenting the standard cc-pVXZ basis sets with two off-center Gaussians placed directly above and below each carbon atom. This addition brings a small and fixed number of primitives to the basis set irrespective of the value of  $X$ ; hence, the extra computational effort is less significant for large basis sets. We used the planar  $C_6$  ring and benzene as our model monomers. We spanned the potential energy surfaces by varying vertical and horizontal separations using increasingly larger basis sets and different methods.

First of all, this augmentation scheme produces linearly independent basis sets. We encountered no convergence problems for the cases we studied. Almost all the characteristics of the potential energy surfaces can be recovered with these basis sets. Coupled with a computationally economical SCS-MP2, it will be possible to study oligomers of larger PAHs and model graphenes. We conclude that our augmented basis sets produce augmented basis set quality results at a reduced cost.

## References

1. Buckingham AD, Del Bene JE, McDowell SAC (2008) The hydrogen bond. *Chem Phys Lett* 463(1–3):1–10
2. Hobza P, Sponer J (1999) Structure, energetics, and dynamics of the nucleic acid base pairs: nonempirical ab initio calculations. *Chem Rev* 99(11):3247–3276
3. Ditzler MA, Otyepka M, Sponer J, Walter NG (2010) Molecular dynamics and quantum mechanics of RNA: conformational and chemical change we can believe in. *Acc Chem Res* 43(1):40–47
4. Asensio JL, Arda A, Canada FJ, Jimenez-Barbero J (2013) Carbohydrate–aromatic interactions. *Acc Chem Res* 46(4):946–954
5. Yilgör E, Yilgör İ, Yurtsever E (2003) Hydrogen bonding and polyurethane morphology. I. Quantum mechanical calculations of hydrogen bond energies and vibrational spectroscopy of model compounds. *Polymer* 43(24):6551–6559
6. Irudayam SJ, Henchman RH (2012) Long-range hydrogen bond structure in aqueous solutions and water-vapor interface. *J Chem Phys* 137(3):034508
7. Hobza P (2008) Stacking interactions. *Phys Chem Chem Phys* 10(19):2581–2583
8. Pumera M, Wong CHA (2013) Graphene and hydrogenated graphene. *Chem Soc Rev* 42(14):5987–5995
9. Müller-Dethlefs K, Hobza P (2000) Noncovalent interactions: a challenge for experiment and theory. *Chem Rev* 100(1):143–167
10. Riley KE, Pitonak M, Jurecka P, Hobza P (2010) Stabilization and structure calculations for noncovalent interactions in extended molecular systems based on wave function and density functional theories. *Chem Rev* 110(9):5023–5063
11. Zhao Y, Truhlar D (2008) The M06 suite of density functionals for main group thermochemistry, thermochemical kinetics, noncovalent interactions, excited states, and transition elements: two new functionals and systematic testing of four M06-class functionals and 12 other functionals. *Theor Chem Accounts* 120(1–3):215–241
12. Aquino AJA, Nachtigallova D, Hobza P, Truhlar DG, Hattig C, Lischka H (2011) The charge-transfer states in stacked nucleobase dimer complex: a benchmark study. *J Comput Chem* 32(7):1217–1227
13. Jansen G, Hesselmann A (2001) Comment on “Using Kohn–Sham orbitals in symmetry-adapted perturbation theory to investigate intermolecular interactions”. *J Phys Chem A* 105(49):11156–11157
14. Grimme S, Antony J, Ehrlich S, Krieg H (2010) A consistent and accurate ab initio parametrization of density functional dispersion correction (DFT-D) for the 94 elements H–Pu. *J Chem Phys* 132(15):154104
15. Grimme S (2003) Improved second-order Møller-Plesset perturbation theory by separate scaling of parallel- and antiparallel-spin pair correlation energies. *J Chem Phys* 118(20):9095–9102
16. Yurtsever E (2010) Stacking of triphenylene: characterization of the potential energy surface. *Theor Chem Accounts* 127(3):133–139
17. Frost AA (1967) Floating spherical Gaussian orbital model of molecular structure. I. Computational procedure. LiH as an example. *J Chem Phys* 47(10):3707–3713
18. Brailsford DF, Hall GG, Hemming N, Martin D (1975) Floating s and p-type gaussian orbitals. *Chem Phys Lett* 35(4):437–440
19. Williams HL, Mas EM, Szalewicz K, Jeziorski B (1995) On the effectiveness of monomer-centered, dimer-centered, and bond-centered basis functions in calculations of intermolecular interactions. *J Chem Phys* 103(17):7374–7391
20. Ding Y, Mei Y, Zhang JZH, Tao FM (2008) Efficient bond function basis sets for pi–pi interaction energies. *J Comput Chem* 29(2):275–279
21. Li P (2012) DFT studies on configurations, stabilities, and IR spectra of neutral carbon clusters. *J At Mol Sci* 3(4):308–322
22. Werner HJ, Knowles PJ, Knizia G, Manby F, Schultz M (2010). MOLPRO, version 2010.1, a package of ab initio programs.
23. Boys SF, Bernardi F (1970) The calculation of small molecular interactions by the differences of separate total energies. Some procedures with reduced errors. *Mol Phys* 19(4):553–566
24. Janowski T, Pulay P (2007) High accuracy benchmark calculations on the benzene dimer potential energy surface. *Chem Phys Lett* 447:27–32
25. Sherrill CD, Sumpter BG, Sinnkrot MO, Marshall MS, Hohenstein EG, Walker RC, Gould IR (2009) Assessment of standard force field models against high quality ab initio potential curves for prototypes of  $\pi$ - $\pi$ , CH/ $\pi$ , and SH/ $\pi$  interactions. *J Comput Chem* 30:2187–2193